Fuel Processing Technology 138 (2015) 629–636

Contents lists available at ScienceDirect

Fuel Processing Technology

journal homepage: www.elsevier.com/locate/fuproc

Mineral sorbents for downstream sodium capture in biomass gasifiers

Lígia Cláudia Castro de Oliveira [a], João Felipe Gonçalves de Oliveira [a], Federico Leandro Greco de Melo [a], Jimmy Degaule Lima Moreno [a], Carla de Araújo Ferreira Melo [b], Antônio Eurico Belo Torres [a], Moises Bastos-Neto [a,*], Diana Cristina Silva de Azevedo [a]

[a] Grupo de Pesquisa em Separações por Adsorção (GPSA), Departamento de Engenharia Química, Universidade Federal do Ceará, Campus do Pici, Bl. 709, 60455-760 Fortaleza, CE, Brazil
[b] PETROBRAS/CENPES, Processos de Conversão de Biomassa, Avenida Horácio Macedo, 950, Ilha do Fundão, 21941-598 Rio de Janeiro, RJ, Brazil

ARTICLE INFO

Article history:
Received 10 April 2015
Received in revised form 30 June 2015
Accepted 4 July 2015
Available online 22 July 2015

Keywords:
Gasification
Biomass
Gas cleaning
Sorption
Sodium
Alkali

ABSTRACT

The concentration of alkali metal vapors (especially sodium and potassium) ordinarily reaches more than 10 ppm during agri-based biomass gasification, leading to several problems, as: corrosion of turbine blades, decreased catalytic activity and undesirable deposition on downstream equipment. Adsorption on aluminosilicates is thought to be an interesting option to reduce alkali concentration in syngas thus generated. Therefore, in this work, six samples of mineral sorbents were exposed to sodium vapors at high temperatures and under moisture conditions. Before and after sodium vapor exposure, samples were characterized by various analytical techniques, textural analysis, TGA, XRD and XRF, aimed at better understanding of the binding mechanisms and assessing their ability to remove sodium from the gas phase. The combination of all techniques allowed the confirmation of the sorption mechanisms, which is chemisorption in most cases, with the formation of silicates and aluminosilicate salts. Sorbents with higher Al content, such as green clay and bauxite, showed potential for the application of capturing alkali metal vapors at high temperatures in the presence of steam by fixing sodium as nepheline ($NaAlSiO_4$). Sorbents with higher silica content (e.g., diatomite and kaolin) showed irreversible fixation of Na, which could not be recovered even upon acid leaching. The presence of elements other than Si and Al (e.g. Ca) also plays an important role in Na sorption.

1. Introduction

The gaseous mixture produced from biomass gasification has been pointed out as a reliable and clean way of producing renewable energy. It contains hydrogen, carbon monoxide, carbon dioxide, methane, aliphatic and aromatic hydrocarbons, as well as impurities [1,2]. Due to the high temperatures required for gasification, alkali metals present in biomass are often released in the product stream. This contamination in the gas phase may be also augmented from other alkali and alkaline earth metal sources present in the gasifier, especially from refractory materials and ceramics used in the cleaning operations of the outlet gas [3].

The concentration of these alkali metals (especially sodium and potassium) can reach more than 10 ppm in syngas obtained from biomass gasification. Salo and Mojtahedi [4] reported that alkali metal concentrations of up to 0.1 ppm wt. may cause corrosion of turbine blades. In addition, alkali metal vapors are known to dramatically decrease the activity of cobalt-supported Fischer–Tropsch catalysts [3]. Some other problems associated with the presence of potassium and chlorine vapors released during the biomass gasification process are [5]: (i) agglomeration in fluidized beds, (ii) reaction between potassium and other components of the ash leading to unwanted substances; (iii) corrosion of the reactor constituent material; (iv) clogging and fouling in pipes; (v) reduction of thermal conversion efficiency and (vi) increase in costs for equipment maintenance. Hence, cleaning the biomass gasifier produced gas is essential to avoid corrosion and deposition of inorganic alkali compounds in downstream equipment. Alkali concentrations must be reduced to acceptable levels according to the destination of the produced syngas.

Several studies have been reported in the literature [6–16] regarding methods and technologies to abate alkali metal vapors in syngas obtained from biomass gasification. Sorption on aluminosilicate-based sorbents has been frequently pointed out as an effective method for this purpose [4,11,17]. The sorption capacity of these materials for alkali vapors at high temperatures depends basically on their composition and physical properties, as well as the water/solid ratio and atmospheric conditions (oxidizing or reducing). Some studies reported in the literature have shown that the presence of water plays a critical role on the occurrence of physical or chemical adsorption [7–10,14–17]. Steam is always present in the gas produced from biomass gasification and therefore the effects of humidity on the sorption of alkali vapors should be carefully taken into account. Most of the previous studies have focused on either the

* Corresponding author.
E-mail addresses: carlaaraujo@petrobras.com.br (C.A.F. Melo), mbn@ufc.br (M. Bastos-Neto).

http://dx.doi.org/10.1016/j.fuproc.2015.07.003
0378-3820/

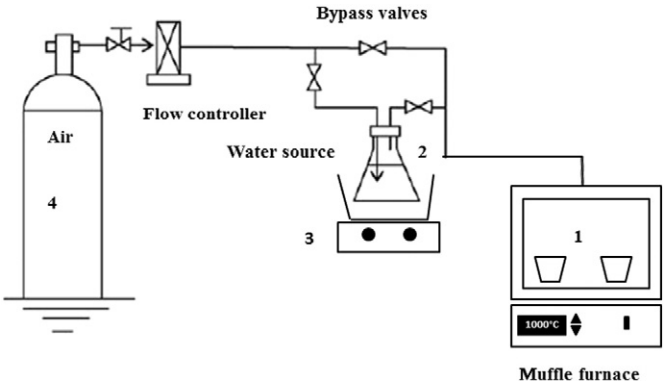

Fig. 1. Experimental apparatus for the gravimetric tests. Legend is as follows: 1 — muffle furnace; 2 — saturator; 3 — heating system; and 4 — air cylinder.

Table 1
Characterization techniques used in this work and their respective purposes.

Technique	Purpose
XRD	Obtain information on the structure and composition of the main phase of the adsorbents and correlate the observed changes due to the exposure to NaCl humid vapors with the adsorption mechanism
XRF	Determine the chemical composition of the sorbents in terms of oxides and identify the effects of the composition (mainly Al_2O_3 and SiO_2) on the adsorption of alkali
SEM/EDS	Detect the presence of sodium on the surface and indicate the occurrence of adsorption by comparing the analysis before and after exposure of the samples to NaCl humid vapors
TGA	Evaluate the thermal stability of the samples under the conditions of test and hydrophilicity/hydrophobicity, which is an important parameter for the analysis of adsorption under humid conditions
ICP-OES	Assess the amount of alkali adsorbed on each sample by comparing the amounts released and irreversibly bound after and before the exposure to NaCl humid vapors

detection of alkali in the gasifier outlet gas or on the selection of sorbents for the removal of alkali metal vapors [6–16]. However, the relation between the retention mechanisms as a function of the solid composition and the presence of water is not fully understood.

The aim of this work is to characterize different sorbents by means of various analytical techniques (XRF, XRD and SEM–EDS) and textural and thermogravimetric analyses, before and after controlled exposure to sodium vapors, in order to shed some light on the sorption mechanisms and to correlate the evaluated characteristics with the sample performance in removing sodium from the gas phase.

2. Experimental

2.1. Materials, reagents and samples

All sorbent samples used in this study are naturally occurring minerals composed of varying amounts of silica (SiO_2) and alumina (Al_2O_3). All samples were kindly supplied by Brasil Minas (Brazil), except bauxite, which was provided by the Department of Geology at the Federal University of Ceará (UFC). All samples were used without prior purification or manipulation.

To minimize risks of contamination, whenever necessary, all plastic and glassware were washed with tap water, immersed in Extran (48 h), rinsed with tap and deionized water and immersed in 20% (v/v) HNO_3 for at least 24 h. Before use, these materials were thoroughly rinsed with ultrapure water.

2.2. Exposure to NaCl humid vapors

The experiments for exposing the fresh mineral sorbents to sodium humid vapors were carried out using sodium chloride as the alkali metal source (5 g NaCl) placed in different crucibles inside a muffle furnace. The samples were heated at a rate of 25 °C min^{-1} up to 1000 °C and kept at this temperature for 5 h inside the muffle. The alkali metal source, NaCl, was purchased from VETEC Química Fina LTDA. (Brazil) and presented >99% purity. A muffle furnace Model EDG 3P-S 3000 (EDG Equipamentos, Brazil) and an analytical balance with 0.0001 g precision Model AB 204-S/FACT — Class I (Mettler Toledo, Brazil) were employed. In order to generate a humid environment inside the muffle furnace, an isothermal water stripper was connected to the system as illustrated in Fig. 1. Deionized water was used in the saturator, which was kept at approximately 80 °C with the aid of a silicon oil bath. The air flow rate was set to 10 $L \cdot min^{-1}$. The steam molar flow rate was 0.0487 kmol water/kmol air, as calculated with the aid of a hygrometer to determine the relative humidity and vapor pressure tables [18].

2.3. Sorbent characterization

All samples were assessed for their textural characteristics before and after exposure to humid sodium vapors by measuring N_2 adsorption isotherms at 77 K in an Autosorb-1 MP apparatus (Quantachrome, USA). From the N_2 isotherms, it was possible to determine the specific surface area, total pore volume and average pore size [19].

X-ray fluorescence analyses (XRF) were performed in an X-ray fluorescence spectrometer ZSXmini II (Rigaku, USA) operating at 40 kV and 1.2 mA. X-ray diffraction (XRD) was carried out on a diffractometer for polycrystalline sample model X'Pert Pro MPD (PANalytical, The Netherlands). The radiation source was a Co X-ray tube, with CoKα operating at 40 kV and 40 mA.

A Sputter Coater POLARON, model SC7620 (VG Microtech, England) was used for SEM–EDS analyses. Samples were mounted in an aluminum holder of 12.7 mm diameter and bombarded with 15 kV from a Leo 440i scanning electron microscope. The characteristic X-rays were detected with an energy-dispersive spectrometer model 6070, calibrated with copper. Both SEM (Leo 440i) and EDS (6070) were purchased from Leo Electron Microscopy Ltd (England). The electron beam current was 50 pA and the measuring time was 10 min.

For thermogravimetric analysis (TGA), a STA 40-9 CD/403/5/G (NETZSCH, Germany) apparatus was employed. The experimental procedure consisted of weighing 30 mg of each sorbent in platinum crucibles. All tests were performed at a heating rate of 20 °C min^{-1}, from room temperature until 850 °C, under an argon (99.999%, supplied by White

Table 2
Composition of the mineral adsorbents obtained by XRF calculated as oxides.

Adsorbents	Mass (%)										SiO_2/Al_2O_3 molar ratio
	Al_2O_3	SiO_2	K_2O	CaO	Fe_2O_3	SO_3	TiO_2	ZrO_2	MgO	MnO	
Bauxite	66.13	20.50	0.11	0.25	7.01	0.19	5.59	0.18	–	–	0.5
Diatomite	4.91	91.96	0.33	0.85	1.12	–	0.79	0.04	–	–	31.8
Green clay	15.65	51.40	6.57	4.74	15.88	0.39	2.10	–	2.43	–	5.6
Kaolin	12.08	75.37	8.75	–	2.31	–	1.36	–	–	–	10.6
Palygorskite	6.05	35.61	0.31	47.3	9.71	–	0.97	0.04	–	–	10.0
Natural zeolite	7.74	45.17	2.01	12.4	4.44	13.7	–	–	–	13.66	9.9

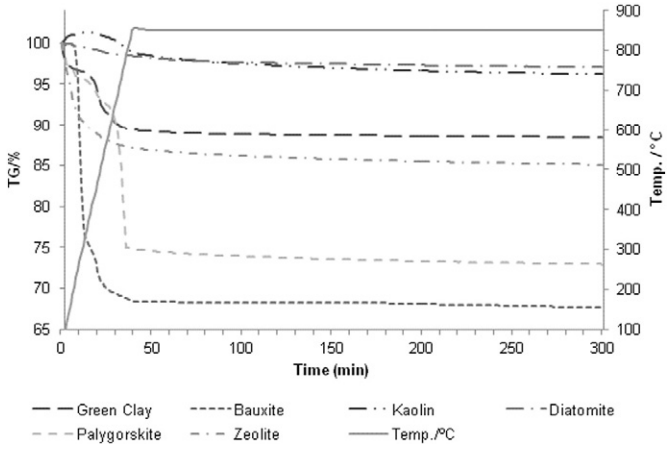

Fig. 2. TG curves of the adsorbents without any pre-treatment: Pt crucible, 20 °C min^{-1}.

Martins Gases Ind., Brazil) flow rate of 20 mL min^{-1}. Each run took 300 min (40 min for temperature rise and 260 min under isothermal conditions).

The fresh and spent samples were also lixiviated (1:5 solid/liquid relation) with a mixture 1:1 of concentrated HCl and HNO_3 acids PA (VETEC Química Fina LTDA., Brazil) for 1 h. Then ICP-OES measurements were performed in the liquid phase in order to evaluate the amount of alkali released and irreversibly bound in each sample. Sodium calibration solutions were prepared from the sodium standard inorganic mono-elementar solution for plasma 100 mg L^{-1} (SpecSol, Brazil). These analyses were carried out on an iCAPICP-OES 6000 series model 300 (Thermo Scientific, USA).

Table 1 summarizes the purposes of applying each characterization technique in the present work. All samples were submitted to each technique before and after exposure to humid sodium vapors, except XRF, which was used only for the fresh materials.

3. Results and discussions

3.1. X-ray fluorescence results

X-ray fluorescence analyses were used to determine the chemical composition of the sorbents in terms of oxides. Table 2 summarizes the results for the samples before their exposure to humid sodium vapors.

The major components detected were SiO_2 and Al_2O_3 in almost every sample, summing up to values above 52%. Palygorskite presented a sum of only 41.7%, which was due to the presence of a high amount (47.3%) of CaO. As a matter of fact, in the fresh sample, calcium is likely to be present as $CaCO_3$, which is converted to CaO at high temperatures and releases CO_2. Bauxite presented the highest alumina content (66.13% in mass) and diatomite the highest silica content (91.96% in mass) and this correlates well with the hydrophobic/hydrophilic character of these samples as discussed afterwards. They showed the highest and lowest total mass losses in TGA experiments (see Fig. 2).

These data may be useful to correlate the molar ratio of SiO_2/Al_2O_3 of the samples with the sodium retention capacity. According to some authors [20], materials with a SiO_2/Al_2O_3 molar ratio near to 8 are promising for the sorption of alkali metal vapor at 1400 °C due to the development of a glass/melt phase [11].

3.2. Thermo-gravimetric analyses

The thermogravimetric curves of the non-pretreated assessed mineral sorbents (Fig. 2) show that bauxite was the material with the most pronounced mass loss relative to its initial mass (31.5%). There was a first mass loss event of 24% in the range of 250–320 °C, corresponding to the loss of water in the form of hydroxyl groups. A second mass loss event of up to 7.5% was observed between 330 and 750 °C, which is attributed to the formation of metastable aluminum oxide [21].

The second greatest mass loss was observed for palygorskite with three distinguished events, adding up to a total mass loss of 25.3%. The first loss of 4% took place at *ca.* 200 °C, due to desorption of weakly bound water molecules. The second event accounting for 3% mass loss at 200–650 °C is related to the dehydration of hydroxyl groups. The third loss (18% at around 800 °C) is probably derived from the conversion of $CaCO_3$ to CaO, as mentioned before and observed in the results of XRD and XRF (to be discussed in the next sections). Calcium carbonate undergoes this reaction and releases CO_2 in a temperature range between about 600 and 800 °C [22].

Natural zeolite presented a continuous mass decrease up to 850 °C, reaching 13% total mass loss. Green clay registered two regions of mass loss. The first, of about 4% up to 220 °C, corresponded to the loss of adsorbed water and the second, of 5%, was probably due to the elimination of water by decomposition of hydroxyl groups [23] in the temperature range between 400 °C and 850 °C.

The lowest total mass losses were observed for kaolin and diatomite, 4% and 2% respectively of the initial mass. Their relatively high silica content accounts for their low hydrophilicity.

3.3. X-ray diffraction results

XRD characterizations were useful to obtain information on the structure and composition of the main phase of the sorbents in their

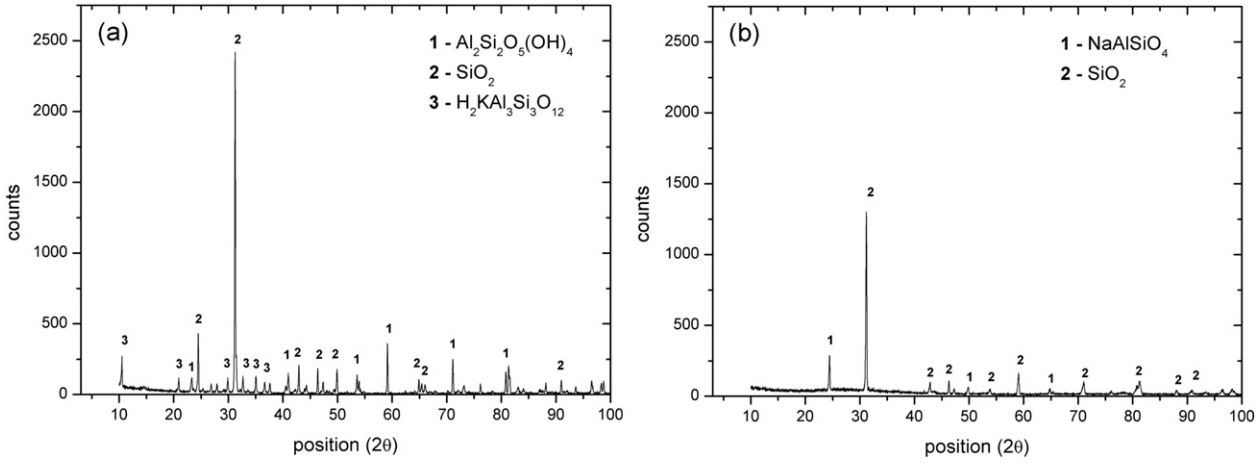

Fig. 3. Diffractograms of fresh kaolin (a) and kaolin after exposure to NaCl humid vapors (b).

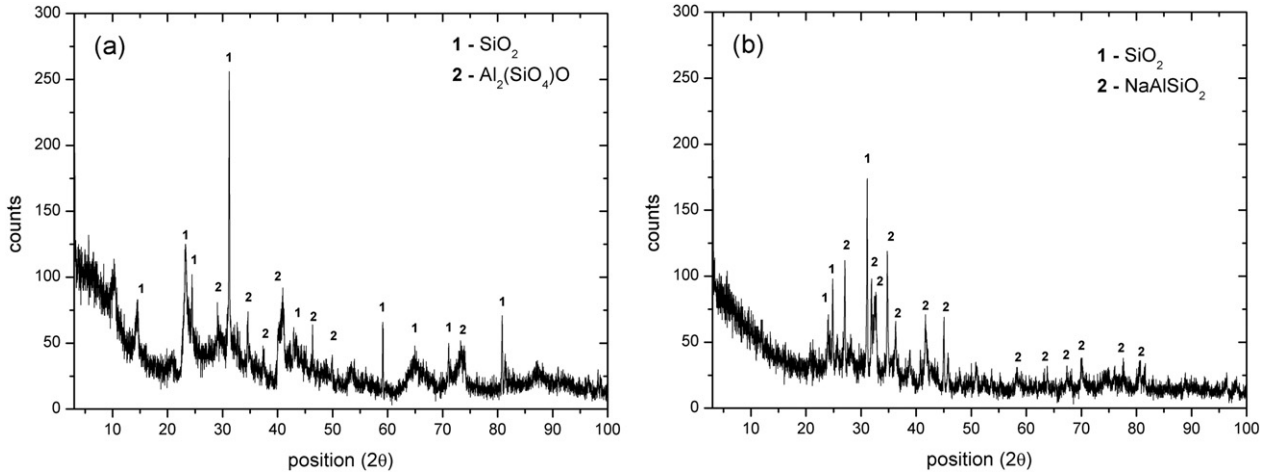

Fig. 4. Diffractograms of fresh green clay (a) and green clay after exposure to NaCl humid vapors (b).

natural form and after exposing them to NaCl humid vapors under high temperature conditions (1000 °C).

Fresh kaolin showed kaolinite ($Al_2Si_2O_5(OH)_4$) and silicon oxide (SiO_2) as main phases and a minor phase corresponding to muscovite ($H_2KAl_3Si_3O_{12}$), which usually occurs with kaolinite and confirms the presence of potassium detected by XRF (Table 2). According to Tran et al. [24], kaolin is composed mainly of kaolinite and when dehydrated at high temperatures it produces $Al_2O_3 \cdot 2SiO_2$. After Na vapor exposure, a $NaAlSiO_4$ phase was detected in the structure, which is attributed to the alkali sorption. The corresponding diffractograms are presented in Fig. 3.

The new phase corresponding to sodium aluminosilicate, $NaAlSiO_4$ (Fig. 3b), occurs when the chemisorption of NaCl in the presence of water takes place, according to the following reaction [11]:

$$2NaCl + H_2O + Al_2O_3 \cdot 2SiO_2 \rightarrow 2NaAlSiO_4 + 2HCl. \quad (1)$$

The presence of steam in the system is responsible for the production of HCl, which is undesirable for the alkali removal process, given the high corrosiveness of this acid. The proposed reaction is consistent with the diffractogram in Fig. 3b because no chloride is detected in the structure after the sorption test.

Analogously, Fig. 4 displays the diffractograms for fresh and spent green clay. The results show that green clay also favors the formation of sodium aluminosilicate, $NaAlSiO_4$, upon exposure to humid Na vapors, indicating that the sorption mechanism (reaction (1)) is the same as for kaolin. In fact, both sorbents have similar alumina content (see Table 2), which seems to play an important role in reaction (1).

The same is not observed for diatomite (see Fig. 5), which is nearly 100% silica. Although previous studies of alkali sorption on diatomaceous earth [13] have revealed the presence of a sodium silicate phase, $Na_2O \cdot 2(SiO_2)$ or $Na_2Si_2O_5$, no relevant evidence was found for such occurrence. The diffractogram of fresh diatomite sample (Fig. 5a) reveals the presence of quartz (SiO_2) in the structure. The exposure of this material to NaCl humid vapors at 1000 °C promoted the formation of a cristobalite phase (also SiO_2, in Fig. 5b) [25]. Minor peaks might be related to the presence of Na, but no conclusion could be made based only on the XRD patterns.

The diffractogram for fresh bauxite (Fig. 6a) showed a well-crystallized structure consisting mainly of gibbsite ($Al_2O_3 \cdot 3H_2O$), followed by silicon oxide. After being exposed to humid sodium vapors, a significant change was observed, not only due to the loss of water but also due to the formation of a sodium aluminosilicate phase called nepheline, $NaAlSiO_4$ (Fig. 6b). The occurrence of this species was also reported by Wolf et al. [15] for the sorption of NaCl vapor on different mineral sorbents.

Moreover, the gibbsite phase in natural bauxite was converted into alumina, which turns into metastable phases of alumina upon heating at high temperatures. The formation of the Al_2O_3 phase, also called corundum, starts at around 1000 °C and reaches a maximum at temperatures above 1100 °C [26,27], which is in accordance with the low intensity of the detected peaks.

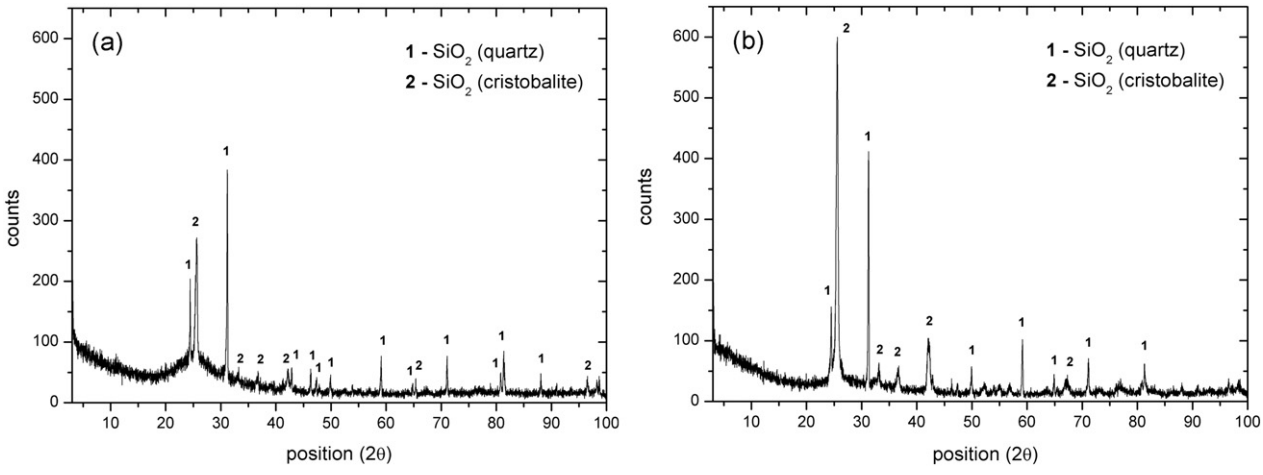

Fig. 5. Diffractograms of fresh diatomite (a) and diatomite after exposure to NaCl humid vapors (b).

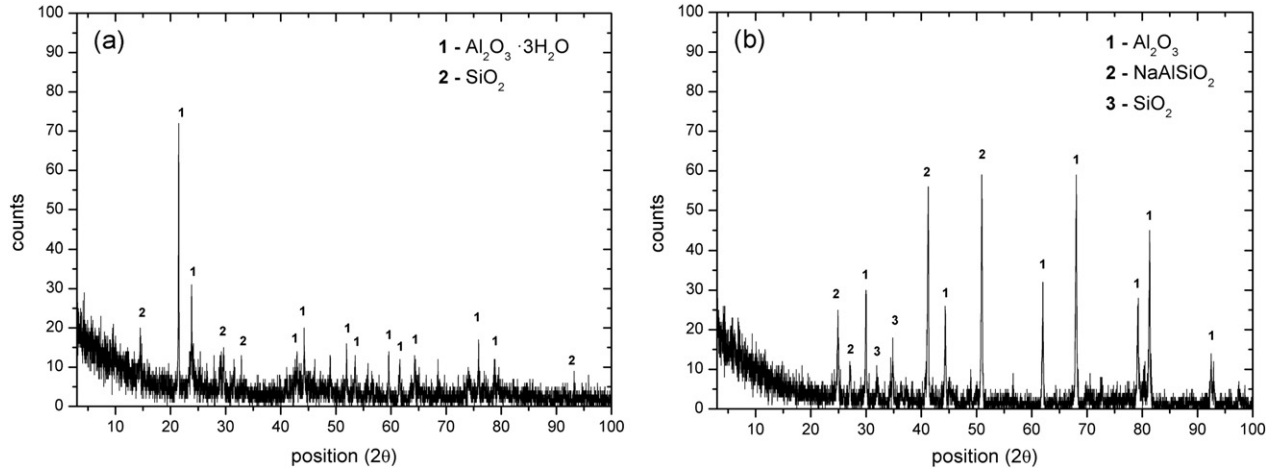

Fig. 6. Diffractograms of natural bauxite (a) and bauxite after exposure to NaCl humid vapors (b).

Palygorskite, also known as attapulgite, is a hydrated clay mineral of magnesium and aluminum with microfibrous morphology and low surface charges [28]. The structure of attapulgite is of 2:1 type with two tetrahedral sheets of silicon oxides joined by a central octahedral sheet of magnesium and aluminum oxides [29]. The diffractogram of fresh palygorskite (Fig. 7a) showed a major phase corresponding to $MgAlSi_4O_{10}(OH)\cdot 4H_2O$, the unit cell composition of palygorskite, and a minor phase of $CaCO_3$. The high crystallinity profile suggests high purity. After contact with NaCl and steam at 1000 °C, a new structure emerges, Ca_2,Na,Mg,Fe,Al($AlSiO_7$), indicating some substitutions of Mg^{+2} and Al^{+3} by Na^{+} and Ca^{+2} as well as Si^{+4} by Al^{+3}, which has been also observed by Cai et al. [30], besides the presence of silicon oxide and material dehydration.

The fresh natural zeolite sample presented only a minor amount of crystalline SiO_2 and no other crystalline component (Fig. 8a), despite the detection of alumina in the FRX analysis. After the gravimetric test (Fig. 8b), a small change has been detected, indicating the formation of crystalline structures of sodium aluminum silicon oxide hydrate Na–Al–Si–O·xH_2O. This suggests that there is indeed alumina in the fresh sample and that the sorption mechanism is the same as that observed for kaolin, green clay and bauxite (Eq. (1)).

As a general trend, X-ray diffractograms suggest that the binding mechanism of sodium in the presence of water is essentially a chemisorption process, regardless of the aluminum or silicon content. In nearly all cases, chemisorption releases HCl, which seems to be the main cause of the accelerated corrosion observed in the muffle furnace walls after vapor exposure experiments.

3.4. SEM–EDS results

Table 3 summarizes the mass composition results obtained by SEM–EDS for the six selected sorbents before and after exposure to Na humid vapors. In spite of being a qualitative method in essence, EDS data have shown that sodium content has been clearly increased after contact with NaCl and steam at 1000 °C, for all cases, thus indicating the occurrence of sorption.

The detection of sodium after the exposure test, as contrasted with its absence in the fresh material (except for zeolite), is indicative of the capacity of these sorbents to retain the alkali metal vapor at high temperatures. In terms of mg Na per g of sorbent, the best results were obtained for green clay and bauxite, which are the materials with the highest Al content and lowest SiO_2/Al_2O_3 ratio. Kaolin and diatomite show a relatively low Al content and retain less sodium, as compared to bauxite and green clay. Palygorskite has an intermediate sodium retention capacity, between the two afore-mentioned groups of sorbents (bauxite/green clay and diatomite/kaolin). Although it has a relatively low aluminum content, sodium retention is believed to be mainly due to the formation of mixed salts of sodium, calcium, magnesium and iron, as demonstrated by XRD.

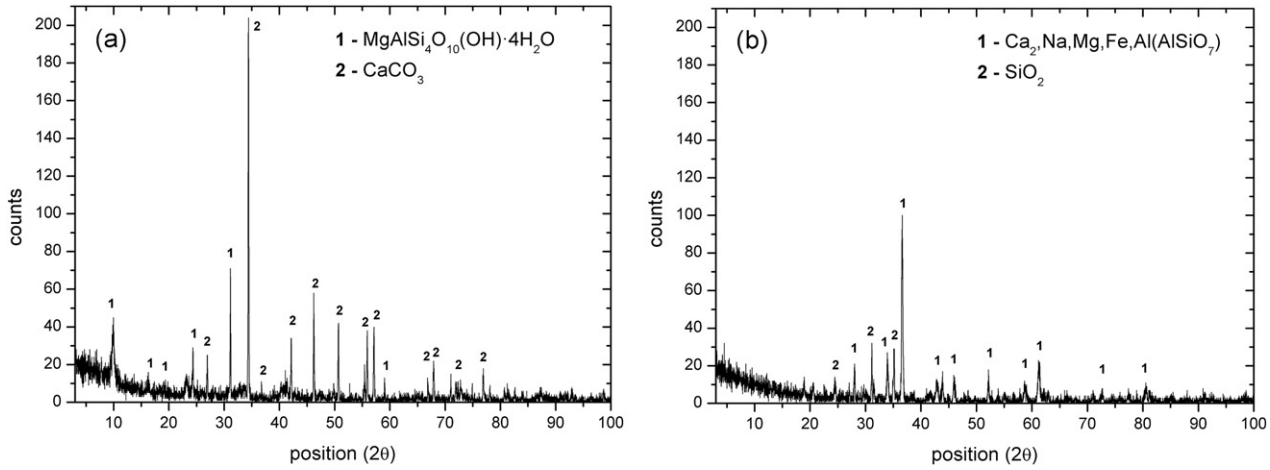

Fig. 7. Diffractograms of fresh palygorskite (a) and palygorskite after exposure to NaCl humid vapors (b).

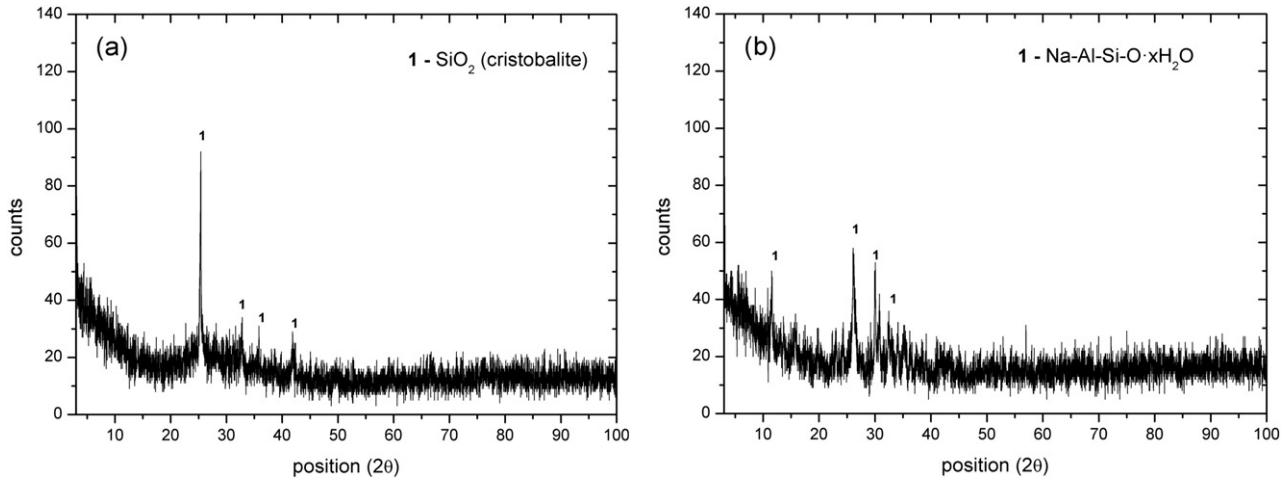

Fig. 8. Diffractograms of fresh natural zeolite (a) and natural zeolite after exposure to NaCl humid vapors (b).

3.5. ICP-OES results

Table 4 summarizes the results of sodium concentration on the sorbents before and after exposure to NaCl humid vapors. Sodium content was determined by partial leaching of desorbable metals on the previously acidified samples. Diluted acids, chelating agents and neutral salts have been commonly used for the extraction of metals, providing data for the evaluation of toxicity and accumulation potential [31]. Diluted acids partially extract trace elements associated with different components as exchangeable carbonates, iron and manganese oxides and organic matter [32]. Nevertheless, such leaching procedure is not often able to dissolve the sample completely. In general, the results shown in Table 4 are consistent with those obtained from the SEM–EDS analyses, although the latter showed higher retention values (except for the zeolite), which suggests that there is indeed a fraction of chemisorbed sodium, which is not recovered by acid leaching. Kaolin and diatomite showed the lowest fractions of leachable sodium, but a relatively high bulk concentration (as determined by SEM–EDS), which suggests that the fixation of sodium on these sorbents occurs mainly by irreversible chemical adsorption. These materials are those with higher silica content.

Although the leaching was only partial, sodium sorption has been also indicated by its concentration after exposure to NaCl vapors, which were considerably higher in comparison with the Na content in the fresh sorbents (without any pre-treatment), especially for green clay, bauxite and natural zeolite. These results are qualitatively representative, but given the fact that the leaching was only partial, one may not conclude that they are quantitatively accurate.

3.6. Textural analysis of samples

The porous texture of the samples was examined in order to determine to which extent it influenced sodium retention capacity. Fig. 9 illustrates the isotherms of nitrogen at 77 K for all samples before being exposed to NaCl vapors. The isotherms were used to determine the specific surface area (S_{BET}), total pore volume (V_T) and average pore diameter (d_p) for the materials before and after the gravimetric tests with NaCl in the presence of steam. Results are shown in Table 5. Kaolin and diatomite presented very low sorption capacity of nitrogen, indicating the presence of little or almost no pores accessible to N_2. The formation of hysteresis in green clay, bauxite, palygorskite and zeolite suggests the presence of mesopores (2 to 50 nm) [19].

The values of specific surface area and total pore volume for kaolin and diatomite were considerably lower than those of the other samples. As a matter of fact, these sorbents showed the lowest Na binding capacities, as determined both from SEM–EDS and leaching tests. On the other hand, bauxite, natural zeolite and green clay have much larger surface areas and would be potentially better sorbents for the removal of alkali vapors. This is in agreement with the results of higher Na retention obtained for bauxite, green clay and even palygorskite, which has an intermediate surface area. The data presented in Table 5 also shows that nearly all of the samples have a null surface area after exposure to NaCl humid vapors, which suggests that sorption of NaCl takes place with the filling or blocking of pores (and eventually interparticle space) of the fresh material.

In other words, the performance of the materials under study for the sorption of humid sodium vapors does not only depend on the texture, but rather on a combination of available surface area and adequate

Table 3
Composition in mass percentage obtained by probe EDS coupled to SEM.

Adsorbents	Mass composition (%)								Na (mg g^{-1})[a]	
	Al		Si		O		Na			
	Before	After	Before	After	Before	After	Before	After	Before	After
Bauxite	26	37	6	7	68	51	0	5	0	49
Diatomite	3	3	47	50	50	44	0	3	0	28
Green clay	12	11	26	24	62	58	0	7	0	68
Kaolin	6	8	33	34	61	56	0	2	0	23
Palygorskite	4	6	16	22	80	69	0	3	0	33
Natural zeolite	4	4	31	21	64	74	1	1	6	7

Before: Fresh sample (without any previous treatment).
After: Sample after exposure to NaCl humid vapors.
[a] Values of Na concentration in mg g^{-1} of sample, considering that the sample consists essentially of silicon and aluminum oxides.

Table 4
Concentrations (±standard deviation, SD) of Na, obtained by ICP OES, in leachates from adsorbent samples (n = 4) before and after exposure to NaCl humid vapors.

Adsorbents	Concentration of sodium (mg g^{-1})		As from SEM–EDS, after exposure
	Before	After	
Bauxite	1.956 ± 0.014	27.393 ± 0.062	49
Diatomite	2.142 ± 0.023	2.504 ± 0.010	28
Green clay	2.895 ± 0.015	40.367 ± 0.014	68
Kaolin	1.736 ± 0.005	2.307 ± 0.058	23
Palygorskite	2.281 ± 0.021	11.687 ± 0.020	33
Natural zeolite	7.865 ± 0.036	21.090 ± 0.008	7

Table 5
Textural characteristics of the adsorbent samples before and after exposure to NaCl humid vapors.

Adsorbents	Before			After		
	S_{BET} (m^2 g^{-1})	V_T (cm^3 g^{-1})	d_p(nm)	S_{BET} (m^2 g^{-1})	V_T (cm^3 g^{-1})	d_p(nm)
Bauxite	197	0.17	3.4	16	0.05	12.5
Diatomite	4	0.07	69.2	0	0	n.a.
Green clay	115	0.23	7.9	0	0	n.a.
Kaolin	3	0.04	51.9	0	0	n.a.
Palygorskite	60	0.27	18.0	0	0	n.a.
Natural zeolite	136	0.17	4.9	0	0	n.a.

surface chemistry, in which case a certain amount of aluminum oxide/hydroxide is believed to enhance chemisorption.

4. Conclusions

By combining different characterization methods, it was possible to conclude that chemisorption is the predominant mechanism of alkali retention on mineral sorbents at conditions of temperature and humidity close to biomass gasification.

Each technique applied in this study for the analysis of surface chemistry (XRD, XRF, ICP-OES and SEM–EDS) has indicated the occurrence of sodium – in different forms, depending on the nature of the sorbent – bound to the surface of the tested samples after their exposure to humid NaCl vapors. These observations are in agreement with the deterioration of the textural properties as sorption takes place.

It has been also verified that the presence of aluminum oxide/hydroxide in the structure of the sorbent seems to play an important role on the alkali retention capacity. Moderate amounts of Al might be the cause for the better sorption performances of green clay and bauxite, which were the samples with the highest aluminum content and lowest SiO_2/Al_2O_3 ratio. Regarding this ratio, no conclusion could be made with respect to previous studies reporting better capacities for values close to 8.

The presence of calcium oxide in the structure is also believed to improve the sorption capacity, as observed for palygorskite, which presented an intermediate sodium retention capacity.

For the very specific case of the natural zeolite, no significant conclusion based on our observations could be raised. Further studies with other characterization techniques might be required to allow for a better understanding of the sorption phenomena on this material at such high temperature.

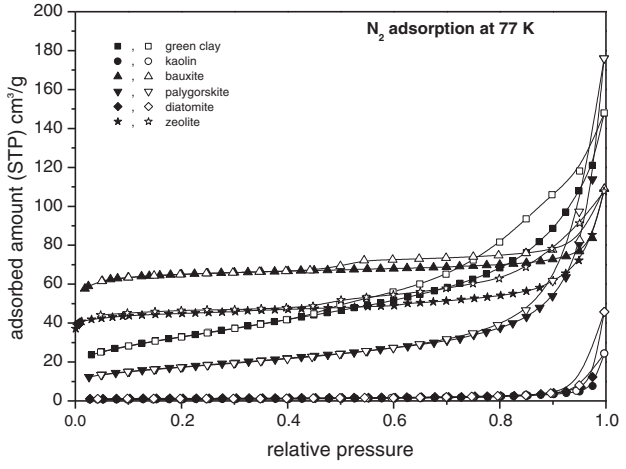

Fig. 9. Adsorption isotherms of nitrogen at 77 K. Filled symbols represent adsorption and open symbols represent desorption data.

Acknowledgments

The authors acknowledge financial support from PETROBRAS (Convênio: 0050.0064627.11.9; SAP: 4600329806).

References

[1] M. Puig-Arnavat, J.C. Bruno, A. Coronas, Review and analysis of biomass gasification models, Renew. Sustain. Energy Rev. 14 (9) (2010) 2841–2851.
[2] A.F. Kirkels, G.P.J. Verbong, Biomass gasification: still promising? A 30-year global overview, Renew. Sustain. Energy Rev. 15 (1) (2011) 471–481.
[3] Ø. Borg, N. Hammer, B.C. Enger, R. Myrstad, O.A. Lindvåg, S. Eri, T.H. Skagseth, E. Rytter, Effect of biomass-derived synthesis gas impurity elements on cobalt Fischer–Tropsch catalyst performance including in situ sulphur and nitrogen addition, J. Catal. 279 (1) (2011) 163–173.
[4] K. Salo, W. Mojtahedi, Fate of alkali and trace metals in biomass gasification, Biomass Bioenergy 15 (3) (1998) 263–267.
[5] K.-Q. Tran, K. Iisa, M. Hagström, B.-M. Steenari, O. Lindqvist, J.B.C. Pettersson, On the application of surface ionization detector for the study of alkali capture by kaolin in a fixed bed reactor, Fuel 83 (7–8) (2004) 807–812.
[6] Y.E. Yudovich, M.P. Ketris, Chlorine in coal: a review, Int. J. Coal Geol. 67 (1–2) (2006) 127–144.
[7] I. Escobar, M. Muller, Alkali removal at about 1400 degrees C for the pressurized pulverized coal combustion combined cycle. 2. Sorbents and sorption mechanisms, Energy Fuel 21 (2) (2007) 735–743.
[8] Y.L. Li, J.A. Li, S.Y. Cheng, W.J. Liang, Y.Q. Jin, Y.Q. Wu, J.S. Gao, Adsorption of NaCl vapor at elevated temperature on mineral adsorbents, Energy Fuel 21 (6) (2007) 3259–3263.
[9] B.L. Dou, W.G. Pan, J.X. Ren, B.B. Chen, J.H. Hwang, T.U. Yu, Single and combined removal of HCl and alkali metal vapor from high-temperature gas by solid sorbents, Energy Fuel 21 (2) (2007) 1019–1023.
[10] B.L. Dou, W.Q. Shen, J.S. Gao, X.Z. Sha, Adsorption of alkali metal vapor from high-temperature coal-derived gas by solid sorbents, Fuel Process. Technol. 82 (1) (2003) 51–60.
[11] I. Escobar, H. Oleschko, K.J. Wolf, M. Muller, Alkali removal from hot flue gas by solid sorbents in pressurized pulverized coal combustion, Powder Technol. 180 (1–2) (2008) 51–56.
[12] T. Takuwa, I. Naruse, Detailed kinetic and control of alkali metal compounds during coal combustion, Fuel Process. Technol. 88 (11–12) (2007) 1029–1034.
[13] S.Q. Turn, C.M. Kinoshita, D.M. Ishimura, J. Zhou, T.T. Hiraki, S.M. Masutani, A review of sorbent materials for fixed bed alkali getter systems in biomass gasifier combined cycle power generation applications, J. Inst. Energy 71 (489) (1998) 163–177.
[14] X.L. Wei, U. Schnell, K.R.G. Hein, Behaviour of gaseous chlorine and alkali metals during biomass thermal utilisation, Fuel 84 (7–8) (2005) 841–848.
[15] K.J. Wolf, M. Müller, K. Hilpert, L. Singheiser, Alkali sorption in second-generation pressurized fluidized-bed combustion, Energy Fuel 18 (6) (2004) 1841–1850.
[16] Y.J. Zheng, P.A. Jensen, A.D. Jensen, A kinetic study of gaseous potassium capture by coal minerals in a high temperature fixed-bed reactor, Fuel 87 (15–16) (2008) 3304–3312.
[17] Y.L. Li, J. Li, Y.Q. Jin, Y.Q. Wu, J.S. Gao, Study on alkali-metal vapor removal for high-temperature cleaning of coal gas, Energy Fuel 19 (4) (2005) 1606–1610.
[18] R.H. Perry, D.W. Green, J.O. Maloney, Perry's Chemical Engineers' Handbook (7th Edition), 7th edition McGraw-Hill, New York, 1997.
[19] F. Rouquerol, J. Rouquerol, K. Sing, Adsorption by Powders & Porous Solids, Academic Press, San Diego, CA, 1999.
[20] W. Willenborg, Untersuchungen zur Alkalireinigung von Heißgasen für Anlagen mit Kohlenstaub-Druckfeuerung, Fakultät für Maschinenwesen, Rheinisch-Westfälischen Technischen Hochschule Aachen (RWTH-Aachen), Emstek 2003, p. 131.
[21] C.M.R. Prado, M.I.R. Alves, M.I.G. Leles, R.I. Medeiros, C.R.N. Otto, F.C. Damasceno, C.H.H. Brait, P.I.B.M. Franco, N.R. Antoniosi Filho, Estudo da ativação ácida e tratamento

térmico de bauxita extraída de jazidas em Minas Gerais, Brasil, Cerâmica 58 (2012) 111–117.
[22] D.A. Skoog, D.M. West, F.J. Holler, Analytical Chemistry: An Introduction, Saunders College Pub., Philadelphia, 1994.
[23] P.S. Santos, 1st ed., Tecnologia de Argilas — Fundamentos, vol. 1, Edgard Blücher, São Paulo, 1975.
[24] K.Q. Tran, K. Iisa, B.M. Steenari, O. Lindqvist, A kinetic study of gaseous alkali capture by kaolin in the fixed bed reactor equipped with an alkali detector, Fuel 84 (2–3) (2005) 169–175.
[25] J.F. Shackelford, R.H. Doremus (Eds.), Ceramic and Glass Materials: Structure, Properties and Processing, Springer Science & Business Media 2008, p. 202.
[26] C. Pascoal, V.C. Pandolfelli, Bauxitas refratárias: composição química, fases e propriedades — Parte I, Cerâmica 46 (2000) 76–82.
[27] C. Pascoal, V.C. Pandolfelli, Bauxitas refratárias: composição química, fases e propriedades — parte II, Cerâmica 46 (2000) 131–138.
[28] A. Neaman, A. Singer, The effects of palygorskite on chemical and physico-chemical properties of soils: a review, Geoderma 123 (3–4) (2004) 297–303.
[29] E. García-Romero, M.S. Barrios, M.A. Bustillo Revuelta, Characteristics of a Mg-palygorskite in Miocene rocks, Madrid basin (Spain), Clay Clay Miner. 52 (4) (2004) 484–494.
[30] Y.F. Cai, J.Y. Xue, D.A. Polya, A Fourier transform infrared spectroscopic study of Mg-rich, Mg-poor and acid leached palygorskites, Spectrochim. Acta A Mol. Biomol. Spectrosc. 66 (2) (2007) 282–288.
[31] J. Liang, J.J. Schoenau, Development of resin membranes as a sensitive indicator of heavy-metal toxicity in the soil environment, Int. J. Environ. Anal. Chem. 59 (2–4) (1995) 265–275.
[32] G. Rauret, Extraction procedures for the determination of heavy metals in contaminated soil and sediment, Talanta 46 (3) (1998) 449–455.